Spectrochimica Acta Part A: Molecular and Biomolecular Spectroscopy 287 (2023) 122063

Contents lists available at ScienceDirect

Spectrochimica Acta Part A: Molecular and Biomolecular Spectroscopy

journal homepage: www.journals.elsevier.com/spectrochimica-acta-part-a-molecular-and-biomolecular-spectroscopy

A modulation method that can improve the performance of LED multi-spectral imaging

Ling Lin [a,b,*], Meiling Fan [a,b], Muhammad Ijaz [a,b], Leiyang Cheng [a,b], Gang Li [a,b]

[a] State Key Laboratory of Precision Measuring Technology and Instruments, Tianjin University, Tianjin 300072, China
[b] Tianjin Key Laboratory of Biomedical Detecting Techniques and Instruments, Tianjin University, Tianjin 300072, China

HIGHLIGHTS:

- Use n square wave signals with the same frequency and phase difference of π/n as carrier signals.
- Realize collecting multi-spectral images with lower carrier occupied bandwidth.
- Reduce the nonlinear error caused by ringing effect and insufficient rotation rate, thus improve the image quality.

GRAPHICAL ABSTRACT

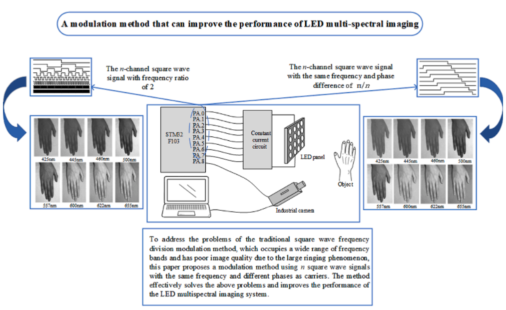

ARTICLE INFO

Keywords:
LED multi-spectral imaging
Ringing phenomenon
Frequency band
Same frequency square wave

ABSTRACT

In the LED multi-spectral imaging (LEDMSI) system, modulation by using the square wave frequency division with frequency ratio of 2 can improve the image quality and acquisition speed, but it will occupy a wide frequency band. Moreover, since there is a simultaneous change in the state of multiple signals when this method is used, it will lead to serious ringing phenomenon or insufficient slew rate and affect the quality of multi-spectral images. To solve the above problems, this paper proposes a modulation method for LEDMSI system, which uses n same frequency square wave signals with different phases as the carrier signals. Comparing the multi-spectral images modulated by the proposed method with the multi-spectral images modulated by the traditional method, experimental results show that the quality of the image modulated by the proposed method is higher, which indicates that the proposed method is of great significance to improve the performance of LEDMSI system.

1. Introduction

At present, there are many different types of multi-spectral imaging technologies and systems [1–9], among them, the LED multi-spectral imaging (LEDMSI) system [6–9] attracts huge attention due to its advantages of high sensitivity and low cost. To improve the acquisition speed of LEDMSI system, researchers have proposed different strategies. Park [10] et al. used a group of light sources and a traditional RGB camera to get images. Shrestha [11] et al. proposed a fast multi-spectral imaging using LED illumination and an RGB camera (RGB-LEDMSI). However, the above studies focus on finding the best combination of LED and the equipment with multi-channel acquisition function to

* Corresponding author at: State Key Laboratory of Precision Measuring Technology and Instruments, Tianjin University, Tianjin 300072, China.
E-mail address: linling@tju.edu.cn (L. Lin).

https://doi.org/10.1016/j.saa.2022.122063
Received 16 August 2022; Received in revised form 9 October 2022; Accepted 29 October 2022
Available online 5 November 2022

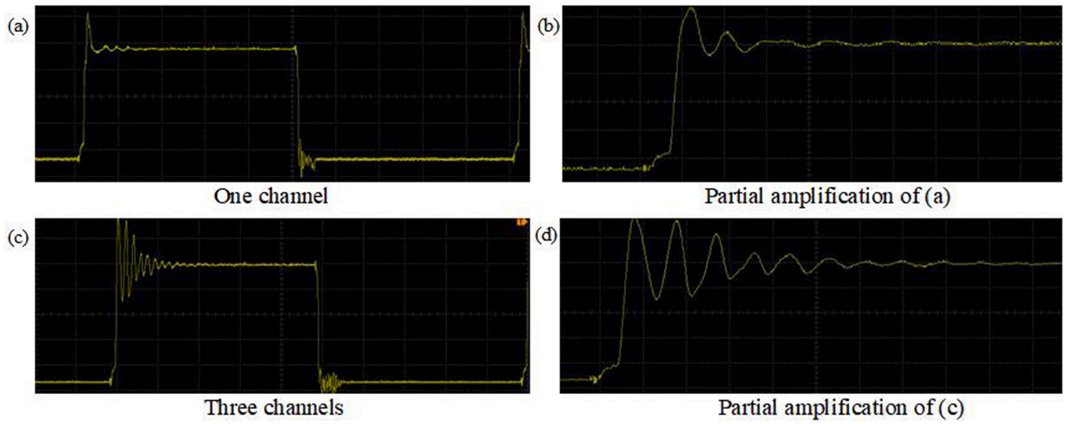

Fig. 1. Square wave signal passing through an underdamped system. Note:(b) and (d) very cell on the x-coordinate represents 10 ms, and very cell on the y-coordinate represents 320mv.

obtain multi-spectral images. This limits the selection of LED band and causes color channel crosstalk. Frequency division multiplexing can realize efficient signal transmission by shifting the signal spectrum to different frequency bands, so many researchers applied it into LEDMSI [12–15]. However, they all used sinusoidal wave as the carrier signal. Because of continuously changing of the amplitude of sinusoidal wave, it is not suitable for integrating mode devices (spectrometers, cameras, analog-to-digital converters (ADC)) with built-in integrator (double integral type ADC, ∑-Δ type ADC, etc.).

The amplitude of square wave signal at its high and low levels remains unchanged, which can make up for the defect of sinusoidal wave as carrier signal, so it has been widely used [16–18]. They all adopted the square wave signal with a frequency ratio of two as the carrier signals, this will aggravate the ringing phenomenon or the insufficient slew rate, thus affecting the signal quality. Therefore, Yang [19] et al. proposed the square wave signal with a frequency ratio of two created by gray code coding to modulate the LED in LEDMSI system, it effectively avoided the problem of large ringing amplitude or insufficient slew rate caused by the simultaneous changes of multiple signal states in the system. However, it did not solve the problem of carrier signals occupied wide frequency range, which will limit the number of signals that can be arranged.

In this paper, by changing the phase of square wave signal, forming n-channel carrier signals with the same frequency and phase difference of π/n. This method realizes the modulation of multi-channel signal with lower occupied frequency band range, and reduces the influence of ringing effect and insufficient slew rate on signal quality at the same time.

2. Theory

2.1. Influence of simultaneous changes of multiple signal states

In the LED driving system based on square wave signal control, it is easy to cause ringing phenomenon or insufficient slew rate. Fig. 1 shows the ringing phenomenon in the system and (a) is the output of square wave signal when only one channel square wave signal state changes, (c) is the output of square wave signal when three channels square wave signals state change simultaneously. In the Fig. 1 (a)(b), the overshoot is about 380mv and the adjustment time is about 20 ms. In the Fig. 1 (c)(d), the overshoot is about 580mv and the adjustment time is about 70 ms. Fig. 2 shows the situation of insufficient slew rate in the system and (a) is the output of square wave signal when only one channel square wave signal state changes, (c) is the output of square wave signal when three channels square wave signal state simultaneously change. In the Fig. 2 (a)(b), the adjustment time is about 1 ms. In the Fig. 2 (c)(d), the adjustment time is about 10 ms. Therefore, it shows that the problem of large ringing amplitude and insufficient slew rate will be aggravated when the number of signals with simultaneous state changes in the system increased.

In the LEDMSI system, in order to improve the signal-to-noise ratio (SNR), the maximum gray scale is usually closed to the full scale. However, the ringing phenomenon will increase the input voltage and the LED light intensity, this will cause the local gray scale of the image exceeded the scale and entered the saturation state, and then leading to the reduction of the image gradient information. Besides, when the square wave signal rises exponentially, due to the weak light intensity, the local gray scale of the image will be in the nonlinear region of the camera, which will also lead to the decrease of the image gradient information.

2.2. Modulation and demodulation of square wave signal with same frequency and different phase

In the traditional square wave frequency division modulation method with frequency ratio of 2, n channels of square wave signals are needed as carrier signals when there are n channels of signals. So, the number of square wave signals with simultaneous state changes can reach n. From the analysis in section 2.1, it can be seen that the simultaneous changes of multi-channel signal states will aggravate the ringing phenomenon and insufficient slew rate, which seriously affecting the image quality. In order to reduce the influence of the modulation process on image quality, it is simpler to improve the modulation method to avoid simultaneous changes in the state of multiple signals than to improve the performance of the driving system.

This paper uses n-channel square wave signals with the same frequency and phase difference of π/n to drive the light source. When the n-channel square wave signals are generated, the I/O state of the microprocessor changes at most once at any time. Compared with the square wave signal with a frequency ratio of two formed by binary coding, the logic confusion from one state to the next state is greatly reduced, and the digital circuit avoids to produce a large spike current pulse. Due to only one signal state changes occur at most after the n-channel square wave signal passes through the circuit system compared with the

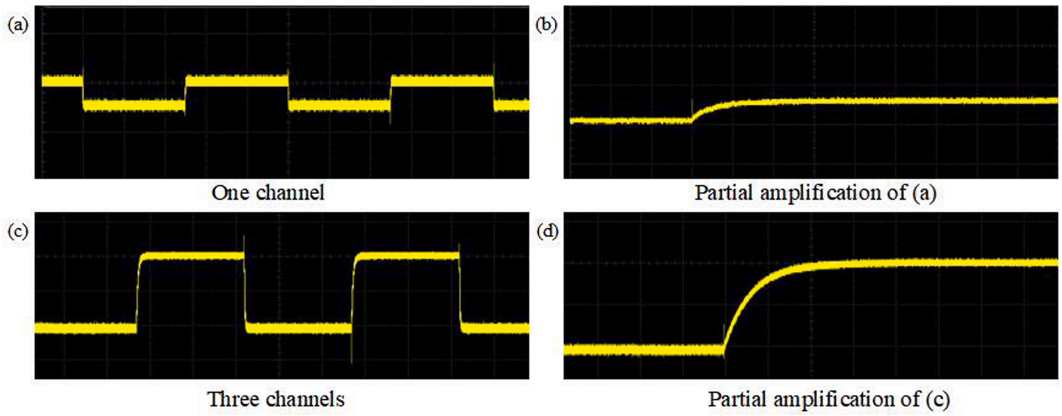

Fig. 2. Square wave signal passing through the damped system. Note:(b) very cell on the x-coordinate represents 1 ms, and very cell on the y-coordinate represents 500mv. (d) very cell on the x-coordinate represents 5 ms, and very cell on the y-coordinate represents 500mv.

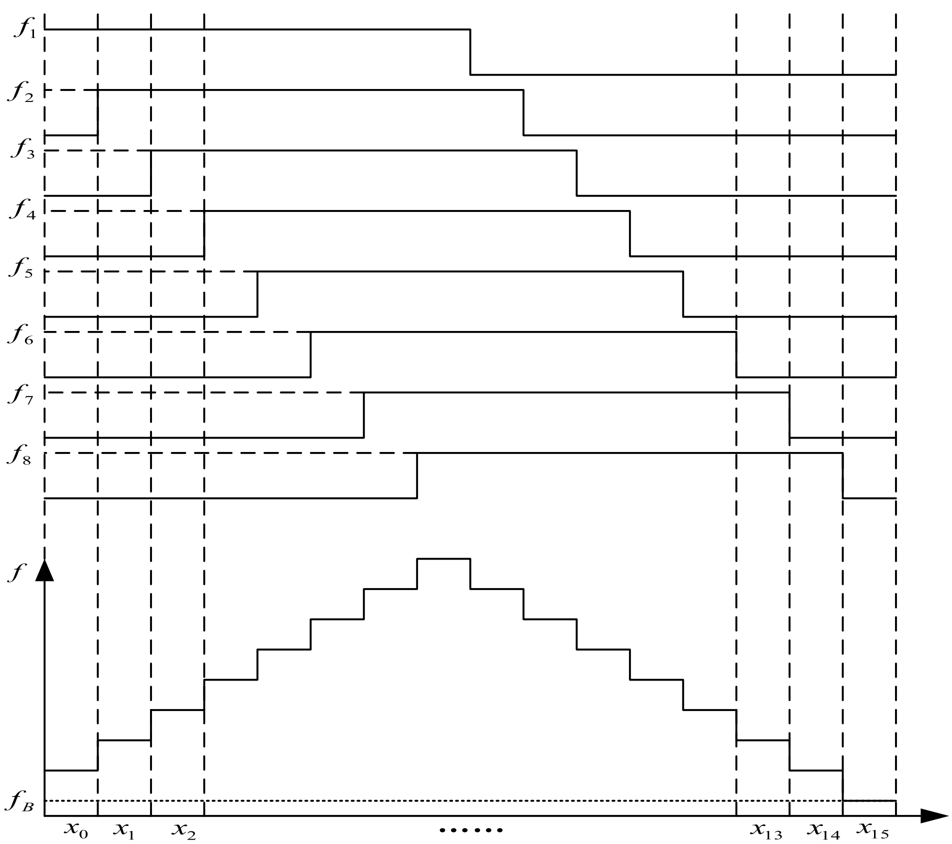

Fig. 3. Sequence of eight channel carrier signal and gray value of one pixel.

traditional square wave frequency division modulation method with frequency ratio of 2, it avoids the simultaneous changes of multi-channel signal states and reduces the problem of large ringing amplitude and insufficient slew rate.

Moreover, since all carrier signals have the same frequency, there will not appear a wide frequency band occupied by the carrier as the number of signal channels increases. Compared with the square wave modulation method with frequency ratio of two, the carrier frequency is reduced by 2^{n-1} times.

Taking the eight-wavelength LEDMSI system as an example, adopt the eight-channel square wave signal with the same frequency and phase difference of π/8 to drive light source. The timing sequences of the eight-channel carrier signals are shown in Fig. 3. Assume that when eight LEDs with different wavelengths work independently, the gray values of the images collected by the camera are $f_1, f_2, f_3, f_4, f_5, f_6, f_7, f_8$ respectively. When the eight LEDs with different wavelengths work according to the timing sequence of carrier signals, the gray value of each frame image collected by the camera in a period is expressed as x_i (i = 0, 1, 2…15) shown in Fig. 3.

Considering the influence of background light, the gray value of each frame image can be expressed as Eq. (1), where f_B is the gray value accumulated by the influence of background light.

$$\left\{\begin{array}{c} x_0 = f_1 + f_B \\ x_1 = f_1 + f_2 + f_B \\ x_2 = f_1 + f_2 + f_3 + f_B \\ x_3 = f_1 + f_2 + f_3 + f_4 + f_B \\ x_4 = f_1 + f_2 + f_3 + f_4 + f_5 + f_B \\ x_5 = f_1 + f_2 + f_3 + f_4 + f_5 + f_6 + f_B \\ x_6 = f_1 + f_2 + f_3 + f_4 + f_5 + f_6 + f_7 + f_B \\ x_7 = f_1 + f_2 + f_3 + f_4 + f_5 + f_6 + f_7 + f_8 + f_B \end{array}\right. \left\{\begin{array}{c} x_8 = f_2 + f_3 + f_4 + f_5 + f_6 + f_7 + f_8 + f_B \\ x_9 = f_3 + f_4 + f_5 + f_6 + f_7 + f_8 + f_B \\ x_{10} = f_4 + f_5 + f_6 + f_7 + f_8 + f_B \\ x_{11} = f_5 + f_6 + f_7 + f_8 + f_B \\ x_{12} = f_6 + f_7 + f_8 + f_B \\ x_{13} = f_7 + f_8 + f_B \\ x_{14} = f_8 + f_B \\ x_{15} = f_B \end{array}\right. \tag{1}$$

If:

$$s = \sum_{i=0}^{15} x_i \tag{2}$$

Then:

$$\left\{\begin{array}{l} 8f_1 = s - 8x_{15} - 8x_8 \\ 8f_2 = s - 8x_0 - 8x_9 \\ 8f_3 = s - 8x_1 - 8x_{10} \\ 8f_4 = s - 8x_2 - 8x_{11} \\ 8f_5 = s - 8x_3 - 8x_{12} \\ 8f_6 = s - 8x_4 - 8x_{13} \\ 8f_7 = s - 8x_5 - 8x_{14} \\ 8f_8 = s - 8x_6 - 8x_{15} \end{array}\right. \tag{3}$$

Through Eq. (3), corresponding image of each wavelength at eight wavelengths can be demodulated. This algorithm can not only eliminate the influence of ambient light, but also carry out frame accumulation [20] to reduce random error (the frame accumulation refers to adding multiple frames of images together). In the eight-wavelength system, one period is 16 frames. When extended to the n-wavelength system, one period is $2n$ frames. The demodulation formula can be expressed as:

$$\left\{\begin{array}{c} nf_1 = s - nx_{2n-1} - nx_n \\ nf_i = s - nx_{i-2} - nx_{n+i-1}, i = 2, 3, \ldots\ldots n \end{array}\right. \tag{4}$$

$$s = \sum_{i=0}^{2n-1} x_i \tag{5}$$

3. Experiments

3.1. Experimental device and parameters

In order to prove the advantages of this method, this paper takes the acquisition of eight-wavelength multi-spectral image as an example and compares the proposed method with the traditional square wave frequency division modulation method. The acquisition device is shown in Fig. 4, which includes the light source drive unit, the signal receiving unit and the signal processing unit. The light source drive unit is composed of the microprocessor (STM32F103V8T6), the constant- current circuit composed of field effect tube (AP2045) and operational amplifier (TLV2316), the P4115 step-down constant current module and the light-emitting diodes (wavelength respectively is: 425 nm, 445 nm, 460 nm, 500 nm, 557 nm, 600 nm, 622 nm, 655 nm). The signal receiving unit is industrial camera (Hikvision MV-CA016-10UM, sensor model: IMX273, resolution: 1440*1080), and the signal processing unit is computer (MATLAB2018a).

When the proposed method is used, the square waves frequency is 2 Hz, and the initial phases of the eight square wave signals are 0, π/8, 2π/8, 3π/8, 4π/8, 5π/8, 6π/8, 7π/8 respectively. When the traditional square wave frequency division modulation method is used, the frequency of the eight square wave signals is 0.125 Hz, 0.25 Hz, 0.5 Hz, 1 Hz, 2 Hz, 4 Hz, 8 Hz, 16 Hz respectively.

3.2. Experimental process

In order to prove that the experimental results are not related to the experimental object and driving circuit, three sets of experiments were carried out. In all experiments, set the frame rate of the camera at 32 frame and collected 1024 images modulated by two methods respectively.

(1) A constant current circuit composed of field effect transistor (FET) and operational amplifiers (OPAMP) is used to drive LED, and the hand is taken as the experimental object. The images obtained by using the traditional modulation method are shown in Fig. 5(a). The images obtained by using the modulation method proposed in this paper are shown in Fig. 5(b).

(2) A constant current circuit composed of FET and OPAMP is used to drive LED, and feathers are taken as the experimental object. The images

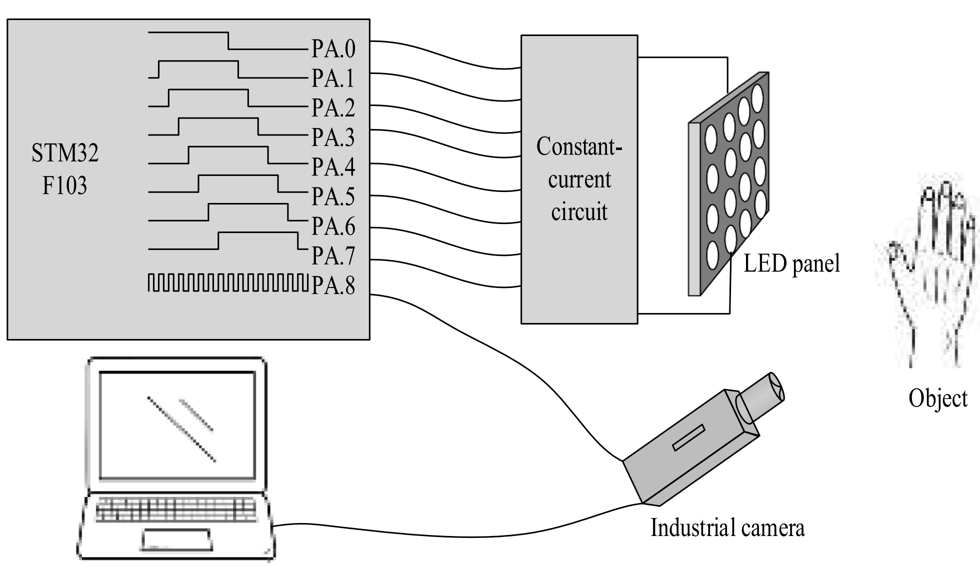

Fig. 4. Experimental device diagram.

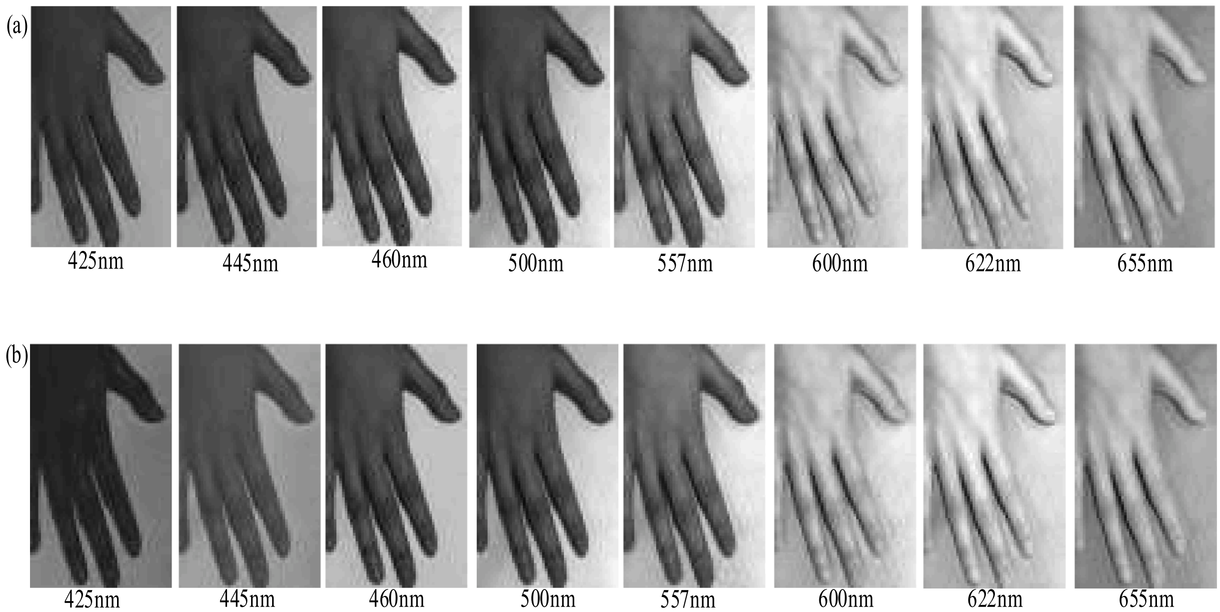

Fig. 5. Images of each wavelength, where (a) is obtained by the method of traditional square wave frequency division, (b) is obtained by the method of traditional square wave frequency division modulation.

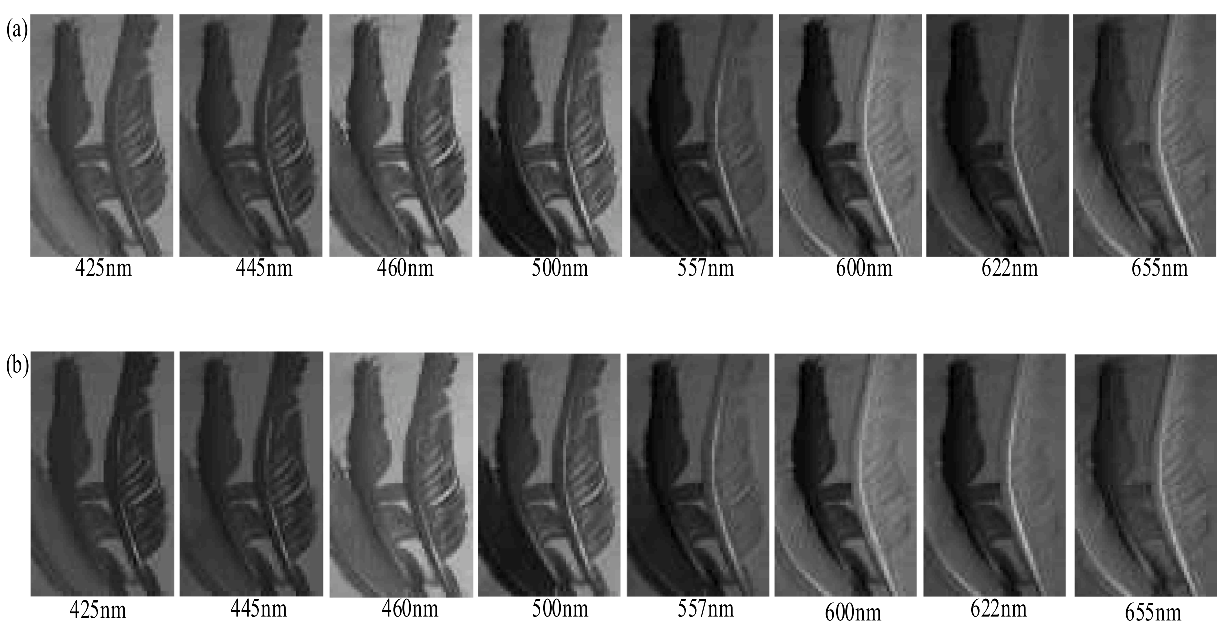

Fig. 6. Images of each wavelength, where (a) is obtained by the method of traditional square wave frequency division, (b) is obtained by the method of traditional square wave frequency division modulation.

obtained by using the traditional modulation method are shown in Fig. 6(a). The images obtained by using the modulation method proposed in this paper are shown in Fig. 6(b).

(3) P4115 step-down constant-current module is used to drive LED, and the hand is taken as the experimental object. The images obtained by using the traditional modulation method are shown in Fig. 7(a). The images obtained by using the modulation method proposed in this paper are shown in Fig. 7(b).

4. Results and discussion

In order to prove that the modulation method proposed in this paper has higher accuracy than the traditional frequency division modulation method, no-reference image quality assessment (NR-IQA) is used to compare the image collected by the two modulation methods. We selected the spatial features (SF) [21], energy of gradient (EOG) and Brenner gradient (Brenner). SF reflects the overall activity degree of an image space, and its expression is shown in Eq. (6). EOG and Brenner are sharpness evaluation indexes based on image gradient, and their expressions are shown in Eq. (7) and (8) respectively.

$$SF=\sqrt{\frac{1}{m\times n}\sum_{i=1}^{m}\sum_{j=2}^{n}[f(i,j)-f(i,j-1)]^2+\frac{1}{m\times n}\sum_{i=1}^{m}\sum_{j=2}^{n}[f(i,j)-f(i-1,j)]^2} \tag{6}$$

$$EOG=\sum_{i}\sum_{j}\{[f(i+1,j)-f(i,j)]^2+[f(i,j+1)-f(i,j)]^2\} \tag{7}$$

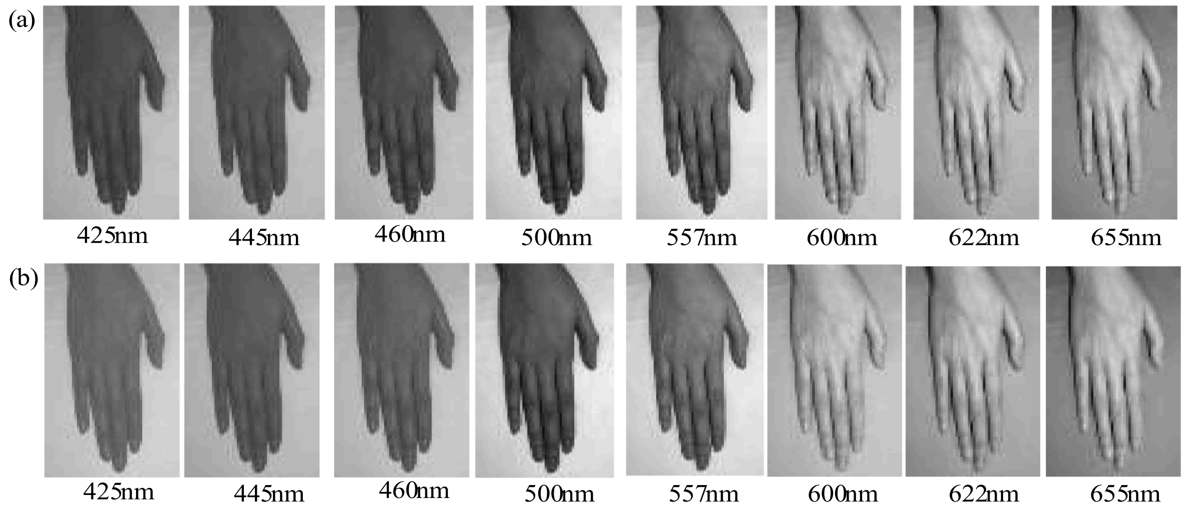

Fig. 7. Images of each wavelength, where (a) is obtained by the method of traditional square wave frequency division, (b) is obtained by the method of traditional square wave frequency division modulation.

Table 1
Quality comparison of images obtained by the modulation method proposed in this paper and traditional square wave frequency division modulation method.

criteria	single-waveband image							
	655 nm		622 nm		600 nm		557 nm	
	1	2	1	2	1	2	1	2
SF	6.06e + 2	6.18e + 2	6.01e + 2	6.67e + 2	2.97e + 2	3.71e + 2	3.83e + 2	4.45e + 2
EOG	5.84e + 10	6.06e + 10	5.74e + 10	7.06e + 10	1.41e + 10	2.18e + 10	2.33e + 10	3.15e + 10
Brenner	5.41e + 10	5.48e + 10	6.09e + 10	7.33e + 10	1.40e + 10	1.95e + 10	2.41e + 10	3.05e + 10
criteria	single-waveband image							
	500nm		460nm		445nm		425nm	
	1	2	1	2	1	2	1	2
SF	7.53e+2	7.88e+2	6.16e+2	6.49e+2	3.92e+2	4.42e+2	4.73e+2	5.11e+2
EOG	9.02e+10	9.85e+10	6.02e+10	6.68e+10	2.44e+10	3.10e+10	3.55e+10	4.14e+10
Brenner	8.68e+10	9.18e+10	4.92e+10	5.30e+10	1.80e+10	2.30e+10	2.42e+10	2.76e+10

$$Brenner = \sum_i \sum_j [f(i+2,j) - f(i,j)]^2 \tag{8}$$

When the traditional square wave frequency division modulation method with a frequency ratio of 2 is used for modulation, there is a situation that multiple signal states change at the same time. However, using the modulation method proposed in this paper, only one signal state changes occurred at most. Therefore, the modulation method proposed in this paper will cause slighter ringing phenomenon and the insufficient slew rate and have less influence on the gradient information of the image. That is, the SF, EOG and Brenner indexes of the image obtained by the modulation method proposed in this paper should be higher.

Table 1 shows the results of SF, EOG and Brenner indexes of images of each wavelength obtained by the two methods when the first experiment in experiment A was conducted. By comparing the results of the three indexes under the two modulation methods, it can be seen that the gradient information of images obtained by using the modulation method proposed in this paper was significantly improved. SF increased by the highest 24.61 % and the lowest 1.86 %. EOG increased by the

Table 2
Quality comparison of images obtained by the modulation method proposed in this paper and traditional square wave frequency division modulation method.

criteria	single-waveband image							
	655 nm		622 nm		600 nm		557 nm	
	1	2	1	2	1	2	1	2
SF	7.49e + 2	7.61e + 2	8.22e + 2	8.36e + 2	3.93e + 2	4.86e + 2	4.51e + 2	4.89e + 2
EOG	8.91e + 10	9.19e + 10	1.07e + 11	1.11e + 11	2.46e + 10	3.76e + 10	3.23e + 10	3.81e + 10
Brenner	8.96e + 10	9.01e + 10	9.66e + 10	1.04e + 11	2.85e + 10	3.82e + 10	3.10e + 10	3.45e + 10
criteria	single-waveband image							
	500nm		460nm		445nm		425nm	
	1	2	1	2	1	2	1	2
SF	8.01e+2	8.42e+2	7.01e+2	7.39e+2	5.47e+2	5.81e+2	5.69e+2	5.94e+2
EOG	1.02e+11	1.13e+11	7.79e+10	8.68e+10	4.75e+10	5.35e+10	5.13e+10	5.60e+10
Brenner	1.15e+11	1.23e+11	7.92e+10	8.46e+10	3.96e+10	4.38e+10	4.42e+10	4.54e+10

Table 3
Quality comparison of images obtained by the modulation method proposed in this paper and traditional square wave frequency division modulation method.

criteria	single-waveband image							
	655 nm		622 nm		600 nm		557 nm	
	1	2	1	2	1	2	1	2
SF	4.91e + 2	5.10e + 2	4.64e + 2	4.69e + 2	2.10e + 2	2.73e + 2	3.14e + 2	3.75e + 2
EOG	5.89e + 10	6.36e + 10	5.26e + 10	5.38e + 10	1.08e + 10	1.83e + 10	2.41e + 10	3.44e + 10
Brenner	3.29e + 10	3.52e + 10	3.22e + 10	3.36e + 10	7.01e + 09	1.12e + 10	1.62e + 10	2.16e + 10
criteria	single-waveband image							
	500nm		460nm		445nm		425nm	
	1	2	1	2	1	2	1	2
SF	7.18e+2	7.59e+2	4.87e+2	5.26e+2	2.79e+2	3.20e+2	2.48e+2	2.88e+2
EOG	1.26e+11	1.41e+11	5.80e+10	6.76e+10	1.90e+10	2.50e+10	1.50e+10	2.03e+10
Brenner	8.21e+10	8.90e+10	4.15e+10	4.75e+10	1.30e+10	1.69e+10	1.01e+10	1.28e+10

Note: 1 means the traditional method, 2 means the proposed method.

highest 54.94 % and the lowest 3.67 %. Brenner increased by the highest 39.15 % and the lowest 1.33 %.

Table 2 shows the SF, EOG, and Brenner index results of images at different wavelengths obtained by the two methods when the second experiment was conducted. Table 1 and Table 2 can prove modulation method proposed in this paper can get higher accuracy signal than the traditional method and the conclusion is not related to the experimental subjects. Table 3 shows the results of three indexes of images of each wavelength obtained by the two methods when the third experiment was conducted. Table 1 and Table 3 can prove modulation method proposed in this paper can get higher accuracy signal than the traditional method and the conclusion is not related to the driving circuit. According to the theoretical analysis and experimental results, the modulation method proposed in this paper can effectively improve the details of multi-spectral images by reducing ringing phenomenon and insufficient slew rate.

5. Conclusion

When using the square wave frequency division modulation method with the frequency ratio of 2 in LEDMSI system, there are two problems: Wide frequency band, thus limiting the number of signals that can be arranged. Ringing phenomenon or insufficient slew rate, thus affecting the image quality. This paper aims at these two problems, proposed a modulation method using n square wave signals with the same frequency and phase difference of π/n as carrier signals. This method realizes collecting multi-spectral images with lower carrier occupied bandwidth. Meanwhile, the nonlinear error caused by ringing effect and insufficient rotation rate is reduced, and improving the image quality. This method can effectively improve the image quality compared with the traditional modulation method. However, the ringing phenomenon and the problem of insufficient slew rate is improved but still exist. It is hoped that with the continuous development of technology, the driving system of LEDMSI system will improve. And combined with the method in this paper can further improve the quality of multi-spectral images.

CRediT authorship contribution statement

Ling Lin: Conceptualization, Methodology. **Meiling Fan:** Investigation, Software, Writing – original draft, Conceptualization, Writing – review & editing. **Muhammad Ijaz:** Writing – review & editing. **Leiyang Cheng:** Resources. **Gang Li:** Supervision.

Funding

This research did not receive any specific grant from funding agencies in the public, commercial, or not-for-profit sectors.

Declaration of Competing Interest

The authors declare that they have no known competing financial interests or personal relationships that could have appeared to influence the work reported in this paper.

Data availability

No data was used for the research described in the article.

Acknowledgement

Thanks to the Key Laboratory of Biomedical Detecting Techniques of Tianjin University for the equipment and support provided.

References

[1] I. Lihacova, A. Derjabo, and J. Spigulis, "A multispectral imaging approach for diagnostics of skin pathologies," in *Conference on Clinical and Biomedical Spectroscopy and Imaging III*, Munich, GERMANY, 2013 May 13-16 2013, vol. 8798, in Proceedings of SPIE, 2013, 10.1117/12.2032491. [L]. Available: <Go to ISI>://WOS:000323834000032.

[2] S. Ortega, H. Fabelo, D. K. Iakovidis, A. Koulaouzidis, and G. M. Callico, "Use of Hyperspectral/Multispectral Imaging in Gastroenterology. Shedding Some-Different-Light into the Dark," J. Clin. Med., vol. 8, no. 1, Jan 2019, Art no. 36, 10.3390/jcm8010036.

[3] J. Qin, K. Chao, M.S. Kim, R. Lu, T.F. Burks, Hyperspectral and multispectral imaging for evaluating food safety and quality, J. Food Eng. 118 (2) (Sep 2013) 157–171, https://doi.org/10.1016/j.jfoodeng.2013.04.001.

[4] W.-H. Su, D.-W. Sun, Multispectral Imaging for Plant Food Quality Analysis and Visualization, Compr. Rev. Food Sci. Food Saf. 17 (1) (Jan 2018) 220–239, https://doi.org/10.1111/1541-4337.12317.

[5] K. Hatzigiannakis, A. Zacharopoulos, X. Zabulis, Multispectral Imaging for the Analysis of Cultural Heritage Objects and Image Registration for Results Optimisation, Ercim News 108 (Jan 2017) 37–38 [Online]. Available: <Go to ISI>://WOS:000392518600024.

[6] N. L. Everdell, I. B. Styles, A. Calcagni, J. Gibson, J. Hebden, and E. Claridge, "Multispectral imaging of the ocular fundus using light emitting diode illumination," *Review of Scientific Instruments,* vol. 81, no. 9, Sep 2010, Art no. 093706, 10.1063/1.3478001.

[7] H. Liu, et al., TuLUMIS - a tunable LED-based underwater multispectral imaging system, Opt. Express 26 (6) (2018) 7811–7828, https://doi.org/10.1364/oe.26.007811.

[8] A.I. Ropodi, E.Z. Panagou, G.-J.-E. Nychas, Multispectral imaging (MSI): A promising method for the detection of minced beef adulteration with horsemeat, Food Control 73 (Mar 2017) 57–63, https://doi.org/10.1016/j.foodcont.2016.05.048.

[9] C. Wang *et al.*, "Multispectral Microimaging System with Narrowband LED Illumination," *Chinese Journal of Lasers-Zhongguo Jiguang,* vol. 47, no. 12, Dec 2020, Art no. 1207006, 10.3788/cjl202017.1207006.

[10] J.-I. Park, M.-H. Lee, M. D. Grossberg, S. K. Nayar, and Ieee, "Multispectral imaging using multiplexed illumination," in *11th IEEE International Conference on Computer Vision*, Rio de Janeiro, BRAZIL, 2007 Oct 14-21 2007, in IEEE International Conference on Computer Vision, 2007, pp. 2049-+. [Online]. Available: <Go to ISI>://WOS:000255099302004.

[11] R. Shrestha, J. Y. Hardeberg, and C. Boust, "LED based multispectral film scanner for accurate color imaging," in *8th International Conference on Signal Image Technology and Internet Based Systems (SITIS)*, Univ Bourgogne, Sorrento, ITALY,

2012 Nov 25-29 2012, 2012, pp. 811-817, 10.1109/sitis.2012.122. [Online]. Available: <Go to ISI>://WOS:000315360300110.

[12] H. Li, G. Li, W. An, G. He, L. Lin, "Synergy effect" and its application in LED-multispectral imaging for improving image quality, Opt. Commun. 438 (2019) 6–12, https://doi.org/10.1016/j.optcom.2018.12.091.

[13] F. Liu, G. Li, W. Yan, G. He, S. Yang, L. Lin, Classification of Heterogeneity on Multi-Spectral Transmission Image Based on Modulation-Demodulation-Frame Accumulation and Pattern Recognition, Ieee Access 7 (2019 2019,) 97732–97744, https://doi.org/10.1109/access.2019.2930296.

[14] Y. Wang, G. Li, W. Yan, G. He, and L. Lin, "Fast demodulation algorithm for multi-wavelength LED frequency-division modulation transmission hyperspectral imaging," *Optik,* vol. 202, Feb 2020, Art no. 163110, 10.1016/j.ijleo.2019.163110.

[15] H. Li, G. Li, Y. Ye, and L. Lin, "A high-efficiency acquisition method of LED-multispectral images based on frequency-division modulation and RGB camera," *Optics Communications,* vol. 480, Feb 1 2021, Art no. 126492, 10.1016/j.optcom.2020.126492.

[16] X. Yang, G. Li, and L. Lin, "Assessment of Spatial Information for Hyperspectral Imaging of Lesion," in *Conference on Optics in Health Care and Biomedical Optics VII*, Beijing, PEOPLES R CHINA, 2017 Oct 12-14 2016, vol. 0024, in Proceedings of SPIE, 2017, 10.1117/12.2245874. [Online]. Available: <Go to ISI>://WOS:000392269600051.

[17] M.A. Mazhar, N.A. Riza, CAOS spectra imager design and advanced high dynamic range FDMA-TDMA CAOS mode, Appl. Opt. 60 (9) (Mar 2021) 2488–2498, https://doi.org/10.1364/ao.417472.

[18] N.A. Riza, M.A. Mazhar, Triple coding empowered FDMA-CDMA mode high-security CAOS camera, Appl. Opt. 60 (26) (Sep 2021) 8154–8163, https://doi.org/10.1364/ao.434322.

[19] Y. Yang, L. Li, M. Zhou, H, Shang, G. Li, L. Lin, "A High-efficiency Acquisition Method of LED multispectral Images using Gray code based square wave frequency division modulation," Digital Signal Processing, vol. 126, no. 1051-2004, Feb 2022 doi:10.1016/j.dsp.2022.103507.

[20] G. Li, H. Tang, D. Kim, J. Gao, L. Lin, Employment of frame accumulation and shaped function for upgrading low-light-level image detection sensitivity, Opt. Lett. 37 (8) (2012) 1361–1363, https://doi.org/10.1364/ol.37.001361.

[21] Z.M.P. Sazzad, Y. Kawayoke, Y. Horita, No reference image quality assessment for JPEG2000 based on spatial features, Sign. Process. Image Commun. 23 (4) (Apr 2008) 257–268, https://doi.org/10.1016/j.image.2008.03.005.